The Effect of Rho-Associated Kinase Inhibition on the Ocular Penetration of Timolol Maleate

John J. Arnold,[1] Mark S. Hansen,[2] Gregory S. Gorman,[1] Toshihiro Inoue,[,2] Vasantha Rao,[2] Simone Spellen,[1] Ronald N. Hunsinger,[3] Christopher A. Chapleau,[1,4] Lucas Pozzo-Miller,[4] W. Daniel Stamer,[2] and Pratap Challa[2]*

Purpose. To assess the effects of Rho-associated kinase (ROCK) inhibition on the intraocular penetration of timolol maleate.

Methods. Ex vivo porcine corneal penetration of timolol maleate, sotalol hydrochloride, or brinzolamide incubated with or without Y-27632 was determined in vertical Franz diffusion cells. The effect of ROCK inhibition on the vasodilation of porcine conjunctival vasculature was assessed by scanning electron microscopy (SEM) and immunohistochemical staining with subsequent laser-scanning confocal microscopy (LSCM). Experiments were conducted in New Zealand White (NZW) rabbits to assess the effect of ROCK inhibition on the intraocular distribution of timolol maleate.

Results. ROCK inhibition resulted in minimal alteration of ex vivo porcine corneal drug penetration of timolol, sotalol, or brinzolamide. SEM and LSCM experiments conducted with conjunctiva and sclera tissue in Franz diffusion cells suggested vasodilation in the conjunctival vasculature in the presence of Y-27632. Pretreatment of the eyes of NZW rabbits with Y-27632 resulted in aggregate fold reductions (1 hour, 0.25-fold; 4 hours, 0.45-fold) of timolol maleate drug concentrations in intraocular tissues (aqueous humor, lens, and iris) versus eyes not receiving Y-27632 pretreatment. Pretreatment with a vasoconstrictor, phenylephrine, resulted in a reversal of the effect of Y-27632 on diminished timolol maleate intraocular penetration in NZW rabbits.

Conclusions. ROCK inhibition reduced the intraocular penetration of administered timolol maleate presumably due to increased systemic elimination through the conjunctival vasculature. It is anticipated that care in order and timing of ROCK inhibitor administration will be warranted for those patients who may be on a multiple topical drug regimen for primary open-angle glaucoma. (*Invest Ophthalmol Vis Sci.* 2013;54:1118–1126) DOI:10.1167/iovs.12-10583

From the [1]McWhorter School of Pharmacy and the [3]Department of Biological and Environmental Sciences, Samford University, Birmingham, Alabama; the [2]Department of Ophthalmology, Duke University, Durham, North Carolina; and the [4]Department of Neurobiology, The University of Alabama at Birmingham, Birmingham, Alabama.

Submitted for publication July 12, 2012; revised September 11 and December 14, 2012; accepted December 26, 2012.

Disclosure: **J.J. Arnold**, None; **M.S. Hansen**, None; **G.S. Gorman**, None; **T. Inoue**, None; **V. Rao**, None; **S. Spellen**, None; **R.N. Hunsinger**, None; **C.A. Chapleau**, None; **L. Pozzo-Miller**, None; **W.D. Stamer**, None; **P. Challa**, None

Current affiliation: *Department of Ophthalmology and Visual Science, Kumamoto University, Kumamoto, Japan.

Corresponding author: John J. Arnold, McWhorter School of Pharmacy, Samford University, 800 Lakeshore Drive, Birmingham, AL 35229; jarnold@samford.edu.

The Rho-associated kinase (ROCK) signaling pathway has recently been extensively studied due to its importance in a myriad of disease states. Inhibition of ROCK has been shown to have therapeutic potential for disease states as diverse as prostate cancer, hypertension, pulmonary hypertension, vasospasm, and stroke.[1–9] ROCK inhibition has also been shown to improve optic nerve blood flow and potently lower intraocular pressure (IOP), both of which would be clinically useful in the treatment of primary open-angle glaucoma (POAG).[10–16] The IOP-lowering effects of ROCK inhibition have been particularly intriguing to the pharmaceutical industry. Presently, several pharmaceutical companies have active programs intended to bring a ROCK inhibitor to market to treat POAG.[17]

Despite being extensively studied, the exact mechanism of action of ROCK inhibition for IOP lowering remains unknown.[18–20] At the cellular level, ROCK activation has been shown to promote actin stress fiber assembly, focal adhesion formation, and contraction in fibroblasts.[21–23] Previous in vitro studies conducted with a specific ROCK kinase inhibitor, Y-27632, have also demonstrated that ROCK inhibition can result in cellular relaxation and loss of cell-substratum adhesions in trabecular meshwork (TM) and Schlemm's canal (SC) cells.[19] Presumably, these effects result in increased paracellular permeability and enhanced aqueous humor outflow between the TM and SC cells. Additionally, Y-27632 has been shown to suppress the carbachol-induced contraction of bovine ciliary muscle.[13] Consequently, ROCK inhibition has resulted in improved outflow facility from perfused bovine and porcine eyes. In vivo, these effects are thought to be responsible for the dramatic and rapid reductions in IOP noted in animal models and now in human clinical trials.

Presently, the in vivo intraocular and extraocular consequences of ROCK inhibition and its impact on ocular drug distribution are not well understood. Due to the vasodilatory effects of ROCK inhibition, the highly vascularized conjunctiva would almost certainly be expected to be physiologically affected. And, indeed, the most troublesome side effect to present thus far in clinical trials with eyedrops containing various ROCK inhibitors has been conjunctival hyperemia and conjunctival hemorrhages.[17] Apart from being an obvious undesired side effect of the use of topically administered ROCK inhibitors, this physiological effect highlights an unanswered question about the clinical use of this class of drugs. The ocular bioavailability of ophthalmic drugs is often very low following topical administration due to the relative impermeability of the cornea and nonspecific extraocular routes of drug loss, which can include nasolacrimal drainage and systemic absorption through the conjunctival vasculature.[24–26] Certainly, any pharmacologic agent that increases blood flow to the conjunctival vasculature would be expected to increase the systemic elimination of concomitantly administered drugs. However, ROCK inhibition could, perhaps, enhance the

Investigative Ophthalmology & Visual Science, February 2013, Vol. 54, No. 2

intraocular penetration of a concurrently administered ocular hypotensive, particularly if it is highly hydrophilic, by increasing paracellular drug permeability through morphological changes induced in corneal epithelial cells. Thus, determining the effect of extraocular ROCK inhibition on intraocular penetration of concurrently administered ocular hypotensives will be important clinical information for future patients who might be on a multiple drug regimen for POAG. Consequently, the purpose of this study is to evaluate the effect of ROCK inhibition on the intraocular penetration of a simultaneously administered ocular hypotensive.

Materials and Methods

Materials

Timolol maleate (≥98%), sotalol hydrochloride (≥98%), and the reagents necessary for scanning electron microscopy (SEM; paraformaldehyde, glutaraldehyde, hexamethyldisilazane) were obtained from Sigma Aldrich (St. Louis, MO). Indomethacin (98%) along with HPLC grade acetonitrile and ammonium acetate were obtained from Fisher (Fair Lawn, NJ). Y-27632 dihydrochloride (>98%) was purchased from Tocris Bioscience (Minneapolis, MN). Brinzolamide 1% suspension was utilized in the commercially available form of Azopt (Alcon, Ft. Worth, TX). Phenylephrine 10% solution was utilized in the commercially available form of AK-Dilate (Akorn, Inc., Somerset, NJ). Naïve rabbit eyes were obtained from Bioreclaimation (Liverpool, NY) and dissected into individual tissues of interest in-house and stored at −80°C.

Ex Vivo Determination of Corneal Drug Penetration in Franz Diffusion Cells

Porcine eyes were obtained from a local abattoir (Thompson's Meat Market, Alexandria, AL). The enucleated eyes were kept on ice during transportation and used within 4 hours of enucleation. Corneas were isolated and suspended in Franz diffusion cells (PermeGear, Inc., Hellertown, PA) which have a diffusional area of 0.64 cm^2 and a receiver chamber volume of 5.1 mL (Fig. 1). Dulbecco's phosphate-buffered saline (dPBS) (pH = 7.0) was placed in the receiver chamber and maintained at 37°C ± 0.5°C and stirred at 600 rpm. Timolol maleate (0.5% w/v), sotalol hydrochloride (0.5% w/v) or brinzolamide (1% w/v) with and without Y-27632 (1% w/v) were mixed in dPBS, and 0.5 mL of each formulation was placed in each of the donor chambers. Samples were taken from the receiver chamber at various time-points and replaced with fresh dPBS. The samples were subsequently stored at −80°C until determination of permeated drug via HPLC analysis.

Quantitative analysis of timolol maleate and brinzolamide was conducted using a HPLC system consisting of a Waters (Milford, MA) 1525 Binary HPLC Pump, a Waters 717 Plus auto injector/auto sampler, a Waters dual absorbance UV detector, and a reversed phase C8 analytical column (Spherisorb, 150 × 4.6 mm internal diameter, 5 μm; Supelco, St. Louis, MO). The mobile phase consisted of potassium phosphate (0.1 M) plus acetonitrile at a ratio of 60:40, respectively, buffered at a pH of 2.5. The mobile phase solution was infused at a flow rate of 1 mL/min. Samples were injected at a volume of 10 μL, and sharp peaks were obtained at retention times of 3.2 (λ = 250 nm) and 3.7 minutes (λ = 294 nm) for brinzolamide and timolol maleate, respectively. Standard preparation solutions consisted of each drug were prepared by serial dilution and measured in triplicate. The squared correlation coefficients for the standard curves (0.0001–0.1 mg/mL) were >0.999 r^2 for both drugs. The interday accuracy of the HPLC method was determined to be 96% to 102.4% while the precision expressed as % CV was <8%. Analysis of sotalol hydrochloride was carried out using liquid chromatography–tandem mass spectrometry (LC-MS/MS) system comprised of a Shimadzu LC-20AD HPLC system using a reverse phase C18 column (Luna, 100 × 2.1 mm, 5-μm particle size; Phenomenex, Torrance, CA). The mobile phase consisted of 5 mM ammonium acetate and acetonitrile each fortified with 0.05% trifluoroacetic acid using a gradient elution profile ramping from 5% to 95% acetonitrile linearly over 3.5 minutes with a flow rate of 400 μL/min and a 10-μL injection volume. Detection was accomplished with an AB Sciex (Foster City, CA) 4000 QTRAP mass spectrometer with electrospray ionization operated in the positive ion mode using mixed reaction monitoring (*m/z* 273.1–213.1). The calibration curve extended from 5 to 1000 ng/mL with a correlation coefficient of 0.9990 and an accuracy of 89% to 107%, while the precision expressed as % CV was <9%.

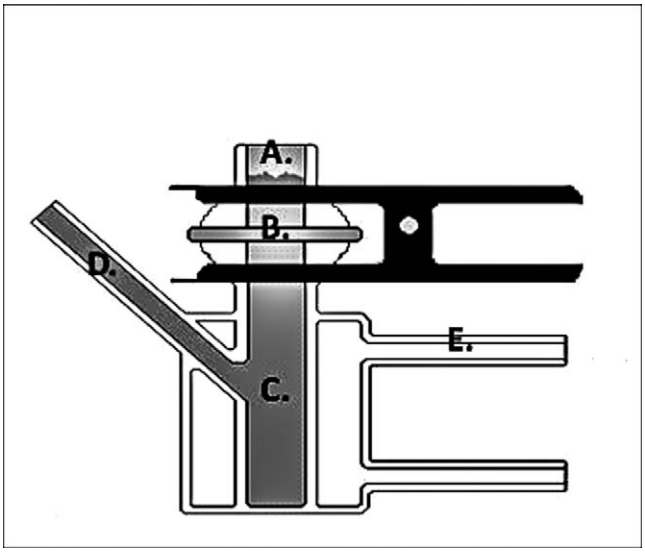

Figure 1. Schematic representation of a Franz diffusion cell utilized for corneal penetration and conjunctival/sclera morphology studies. (**A**) Donor chamber; (**B**) mounted cornea or conjunctiva/sclera; (**C**) receiver chamber; (**D**) sampling port; (**E**) water-jacketed temperature control.

The drug penetration in Franz diffusion cell experiments was assessed as the slope of mcg/sec appearing in the receiver chamber. The apparent permeability coefficient (P_{app}) was calculated from the following equation:

$$P_{app}(cm/sec) = (F \times V_D / SA \times M_D)$$

where F is the drug flux, SA is the surface area for transport, V_D is the donor volume, and M_D is donor amount at time (t) = 0.[27] All data represent the mean of four diffusion cells.

Ex Vivo Scanning Electron Microscope Analysis and Staining of Conjunctival Blood Vessels with Antihuman CD31 (PECAM-1)

Conjunctiva and sclera tissue from porcine eyes was isolated and secured within Franz diffusion cells. Approximately 0.5 mL of timolol maleate (0.5% w/w) with and without Y-27632 (1% w/w) was mixed in dPBS and placed on top of the tissue within the donor compartment. For scanning electron microscopy, the conjunctiva and sclera tissue samples were recovered after 4 hours and fixed in half-strength Karnovsky's glutaraldehyde overnight at 4°C.[28] They were then washed in 0.1 M cacodylate buffer for 15 minutes before being postfixed for 2 hours in 2% aqueous osmium tetroxide. After postfixation the tissue samples were treated with a graded ethanol bath and then soaked for 10 minutes in 100% hexamethyldisilazane for desiccation and allowed to air dry over night under the hood. They were consequently gold coated and photographed using a JEOL JSM-5610LV model scanning electron microscope (JEOL USA, Inc., Waterford, VA) operated at 4 kV.

For laser-scanning confocal microscopy, the conjunctiva and sclera tissue samples were recovered after 4 hours and fixed by immersion in

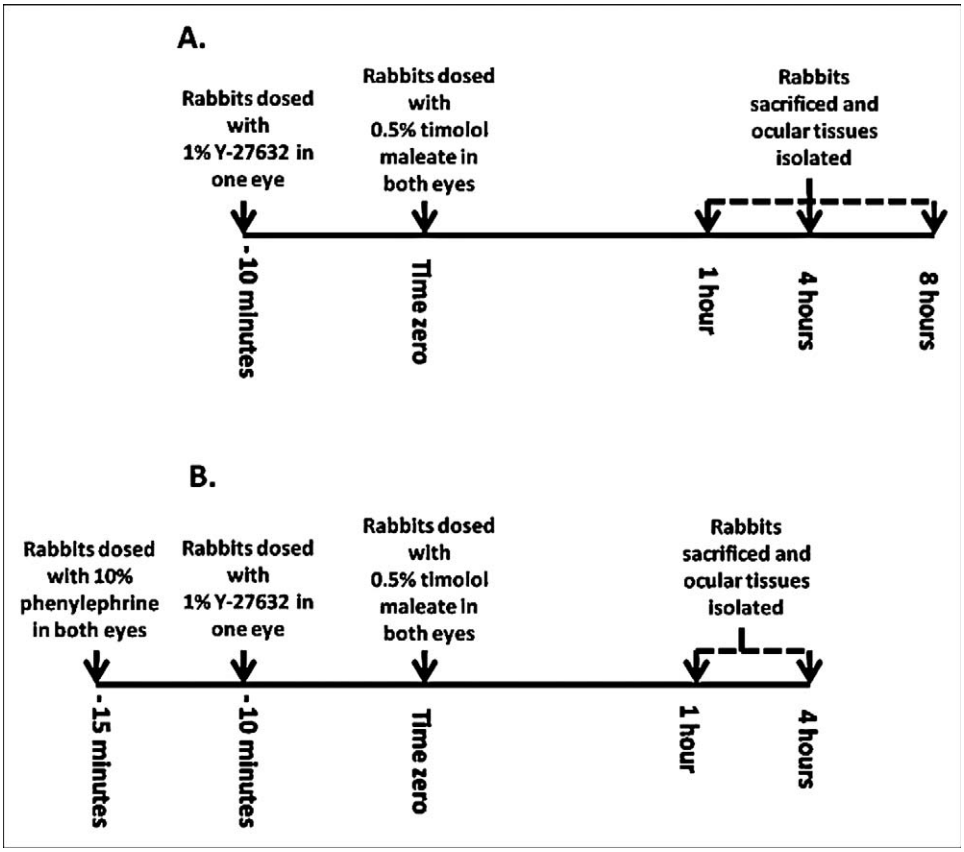

Figure 2. Experimental design of in vivo intraocular timolol maleate penetration studies.

4% paraformaldehyde overnight at 4°C and washed in phosphate-buffered saline (PBS). After the PBS wash, the tissue was then sectioned at 200-μm thickness with a vibratome (Ted Pella Inc., Redding, CA). To determine blood vessel distribution, tissues were stained with the mouse antihuman CD31 (PECAM-1) monoclonal antibody (Cell Signaling Technology, Inc., Danvers, MA). The tissue was permeabilized and blocked with 10% goat serum, 2% bovine serum albumin, and 0.25% Triton-100 in PBS overnight at 4°C. Subsequently, the tissues were incubated overnight (4°C) in primary mouse antihuman CD31 antibodies (dilution 1:150) and then washed in PBS and incubated overnight (4°C) in Alexa Fluor 594 goat antirabbit IgG (dilution 1:150; Invitrogen, Carlsbad, CA). Each tissue sample was then mounted with Vectashield (Vector Laboratories, Burlingame, CA) to prevent photobleaching. Images were acquired with a Fluoview FV-300 laser-scanning confocal microscope (Olympus, Center Valley, PA) using a 10× objective lens. Alexa Fluor 594 was excited using a HeNe laser (647 nm) and detected using standard TRITC dichroic and emission filters (Semrock, Lake Forest, IL). Series of optical sections in the *z*-axis were acquired with 5-μm intervals and displayed as maximum-intensity projections.

In Vivo Rabbit Experiments

Male New Zealand White (NZW) rabbits (3–5 kg) were obtained from Charles River Laboratories (Wilmington, MA). The design of the in vivo rabbit experiments is depicted in Figure 2. The volume of each administered drug solution described was 20 μL. Initially, rabbits were treated topically with eyedrops containing Y-27632 (1% w/v) in one eye as depicted in Figure 2A. Eyedrops containing normal saline were administered as sham treatments to the non–Y-27632-treated eye. Ten minutes later, the rabbits were treated with timolol maleate (0.5% w/v) in both eyes. A different set of animals received initial treatment with phenylephrine (10% w/v) in both eyes (Fig. 2B). Five minutes later, one eye was treated with Y-27632 (1% w/v) with sham treatment of normal saline administered to the contralateral eye. Ten minutes post Y-27632 treatment, the rabbits were administered timolol maleate (0.5% w/v) in both eyes.

For either protocol, the animals were overdosed with pentobarbital and sacrificed via exsanguination at each time-point. Postmortem, rabbit eyes were enucleated and dissected carefully to isolate individual ocular tissues including the aqueous humor, iris, and lens. Tissues were stored at –80°C until eventual determination of drug tissue concentration. The animal studies were conducted per the ARVO Statement on the Use of Animals in Ophthalmic and Vision Research.

Determination of Ocular Tissue Concentrations of Y-27632 and Timolol Maleate

Tissue levels were measured using liquid-tandem mass spectrometry (LC-MS/MS) analysis. The LC-MS/MS system consisted of an AB Sciex 4000 QTRAP tandem mass spectrometer equipped with a Turbo V electrospray ionization (ESI) source and a Shimadzu (Kyoto, Japan) gradient HPLC system. Instrument control and data acquisition was performed with Analyst software version 1.5.1 (AB Sciex).

An Aquasil C18 column (100 mm × 2.1, 5-μm particle size; Thermo Fisher Inc. Waltham, MA) and C18 guard cartridge were used at ambient temperature for separation of the various analytes. The mobile phase consisted of deionized water (A) and acetonitrile (B) both fortified with 0.05% trifluoroacetic acid. A gradient profile with a flow rate of 400 μL/min starting with 95:5 (A/B) for 1.5 minutes and increasing linearly to 10/90 (A:B) over 4 minutes with a 0.5-minute hold before returning the starting mixture and re-equilibrating for 4 minutes. The injection volume was 5 μL, and the analysis time was 10 minutes per sample. The mass spectrometer (4000 QTRAP; AB Sciex) was operated in the positive ion mode (ESI voltage 5 kV and 450°C), and conditions were optimized for each analyte. Multiple reaction

monitoring was used to detect the mass transitions for Timolol (*m/z* 317.2 → 261.2), Y-27632 (*m/z* 213.1 → 95.1), and the internal standard indomethacin (*m/z* 358.1 → 138.9). Nitrogen was used as the curtain and collision gas. Individual stock solutions (1 mg/mL) of timolol maleate and Y-27632 were prepared in 50:50 5 mM ammonium acetate/acetonitrile and indomethacin in acetonitrile. Spiking solutions of Timolol and Y-27632 were prepared by serial dilution of the working stock solution to produce concentrations of each analyte from 10 to 10,000 ng/mL. Indomethacin internal standard spiking solution was prepared at a final concentration of 10 μg/mL. The accuracy of the LC-MS method over the calibration range of 10 to 10,000 ng/mL was determined to 98.8% to 106% and the % CV was less than 10% based on back-calculated values of calibration standards and QC samples.

Naïve eyes from NZW rabbits were dissected into various ocular tissues. The aqueous humor and lens were pooled and homogenized 1:5 (wt/v) and the iris 1:10 (w/v) in 5 mM ammonium acetate buffer. Calibration standards were prepared over a range of 10 to 10,000 ng/mL. Samples were prepared by homogenizing each tissue with 5 mM ammonium acetate as described above. A 100-μL aliquot of each sample was spiked with 10 μL of internal standard spiking solution and extracted with 500 μL of 50:50 5 mM ammonium acetate/acetonitrile followed by vortexing for 30 minutes on a platform shaker and subsequent centrifugation for 5 minutes at ~14,000*g*. The supernatant was transferred into an autosampler vial and cap for analysis.

Results

Effect of ROCK Inhibition on the Corneal Permeability Barrier

Ex vivo studies were conducted in Franz diffusion cells (Fig. 1) to determine the effects of Y-27632 on the porcine corneal penetration of two clinically utilized ocular hypotensives. Initially, timolol maleate was formulated with Y-27632 and without Y-27632 and placed in the donor chamber of the diffusion cells. In the absence or presence of Y-27632, timolol began to appear in the receiver chamber of the diffusion cells at the earliest time-point sampled and consistently increased throughout the course of the experiment (Fig. 3A). After 9 hours, the amount of timolol that had penetrated the cornea in the absence of Y-27632 was 106.5 ± 28.4 μg versus the amount that had penetrated the cornea in the presence of Y-27632 (93.9 ± 34.2 μg). Apparent permeability coefficients (P_{app}) were then calculated for comparison and appear in Figure 3B. Subsequently, a similar corneal penetration study was conducted with another ocular hypotensive. Brinzolamide was incubated in the donor chamber of the diffusion cells with Y-27632 or without Y-27632. Brinzolamide began to appear in the receiver chamber of the diffusion cells at 1 hour and steadily increased throughout the course of the experiment (Fig. 3C). After 9 hours, the amount of brinzolamide that had penetrated the cornea in the presence of Y-27632 was 52.8 ± 9.8 μg versus the amount that had penetrated in the absence of Y-27632 (43.4 ± 5.3 μg). As with the timolol maleate experiments, P_{app} was calculated for comparison and appears in Figure 3D. Additionally, an ex vivo diffusion cell experiment was conducted with sotalol hydrochloride formulated with and without Y-27632 (Fig. 3E). Sotalol is a highly hydrophilic drug which primarily penetrates the cornea via the paracellular pathway.[29] After 9 hours, the amount of sotalol that had penetrated the cornea in the presence of Y-27632 was 78.7 ± 22.5 μg versus the amount that had penetrated in the absence of Y-27632 (76.5 ± 37.5 μg). The P_{app} was calculated for comparison and appears in Figure 3F.

Effect of ROCK Inhibition on Vasodilation of Conjunctival Microcirculation

Vasculature alterations, as a result of a ROCK specific inhibition, were assessed in conjunctiva and sclera tissue from porcine eyes. The tissues were isolated as a single tissue and secured in the Franz diffusion cells. Subsequently, the tissues were incubated with and without Y-27632 for approximately 4 hours and fixed and prepared for SEM. Representative micrographs are presented in Figure 4. Conjunctival blood vessels were visualized in the tissues not treated with Y-27632 (Fig. 4A). However, the tissues treated with Y-27632 appeared to display a more distinctive and prominent conjunctival microvasculature (Fig. 4B).

In order to further clarify these alterations in blood vessel morphology, immunohistochemical staining for the blood vessel–specific antigen CD31 (PECAM-1) was subsequently assessed in a separate set of conjunctiva and sclera tissues. PECAM-1 is hypothesized to function in the endothelium to respond to mechanical changes, such as sudden changes in blood flow.[30,31] Qualitative analysis demonstrated that CD31 expression was highly up-regulated in tissues treated with Y-27632 (Fig. 5). Furthermore, in all samples, the staining of CD31 on Y-27632-treated tissues was highly concentrated along the length of blood vessels, while CD31 staining on control samples was more diffusely distributed.

Effect of ROCK Inhibition on Intraocular Timolol Penetration

In vivo studies in rabbits were conducted in order to determine the effect of ROCK inhibition on the intraocular penetration of timolol. NZW rabbits were administered eyedrops containing Y-27632 in one eye 10 minutes prior to time zero. Rabbits were then administered timolol maleate in both eyes at time zero and then sacrificed at 1, 4, or 8 hours (Fig. 2A). Tissues were collected from the anterior chamber of the eyes of each the animals in order to assess ocular pharmacokinetics and determine if pretreatment with the ROCK inhibitor resulted in an alteration of the intraocular penetration of timolol. In the eyes pretreated with Y-27632, the highest intraocular tissue concentrations for either Y-27632 or timolol were found in the iris at each time-point. Little to none of either drug was found to penetrate to the lens. However, a difference was noted in the pharmacokinetic profiles of the two ocular hypotensives (Fig. 6). The highest tissue concentrations of timolol was noted at 1 hour for each of the tissues evaluated (iris, 2314 ± 1036 ng/mg; aqueous humor, 2019 ± 834 ng/mg; lens: 59 ± 22 ng/mg; Fig. 6A). The tissue concentrations of timolol dropped at 4 hours and were below detectable levels by 8 hours. A similar pharmacokinetic profile was noted for timolol in the contralateral eyes of the animals which were not pretreated with Y-27632 (data not shown). Conversely, the highest tissue concentrations of Y-27632 was noted at 4 hours (iris, 1050 ± 257 ng/mg; aqueous humor, 472 ± 53 ng/mg; lens, 72 ± 9 ng/mg) with the drug persisting in the iris and aqueous humor at 8 hours (Fig. 6B).

Subsequently, the ocular tissue concentrations of timolol of the eyes receiving pretreatment with Y-27632 eyes were divided by the contralateral eye that did not receive pretreatment with Y-27632 eyes and these values were averaged (Fig. 7). Thus, values less than one indicate a relative reduction in timolol concentration in the tissue at that time-point. Pretreatment with Y-27632 resulted in an average fold reduction in all tissue evaluated at 1 hour (Fig. 7A) and 4 hours (Fig. 7B). In the aggregate, there was an approximate 0.25-fold reduction in timolol ocular tissue concentration among the three tissues at 1 hour and an approximately 0.45-fold

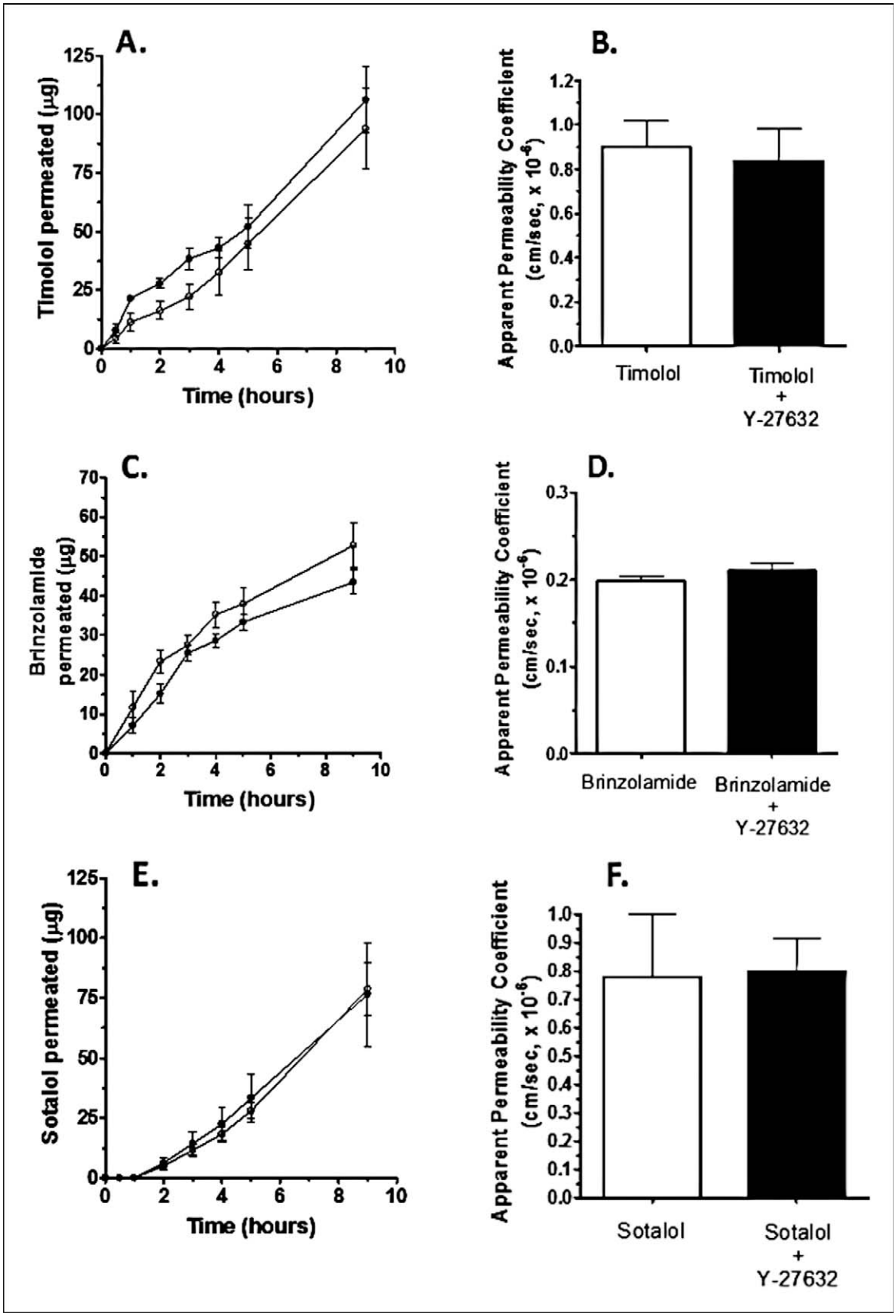

Figure 3. Franz cell diffusion experiments conducted with the ocular hypotensives (**A**) timolol maleate 0.5% w/v, (**C**) brinzolamide 1% w/v, and (**E**) sotalol 0.5% w/v in the absence (*filled circle*) or presence of Y-27632 1% w/v (*open circle*). Data are expressed as mean ± standard deviation ($n = 4$) of total micrograms of ocular hypotensive penetrated versus time. (**B**, **D**, **F**) Apparent permeability coefficients calculated from the data in (**A**, **C**, **E**), respectively. Data are expressed as mean ± standard deviation ($n = 4$).

Figure 4. Scanning electron micrographs of porcine conjunctiva/sclera tissue incubated for 4 hours in Franz diffusion cells in the absence (**A**) or presence (**B**) of Y-27632 (1% w/v). *Arrows* indicate blood vessels. *Magnification*: ×1000, *scale bar*: 10 microns.

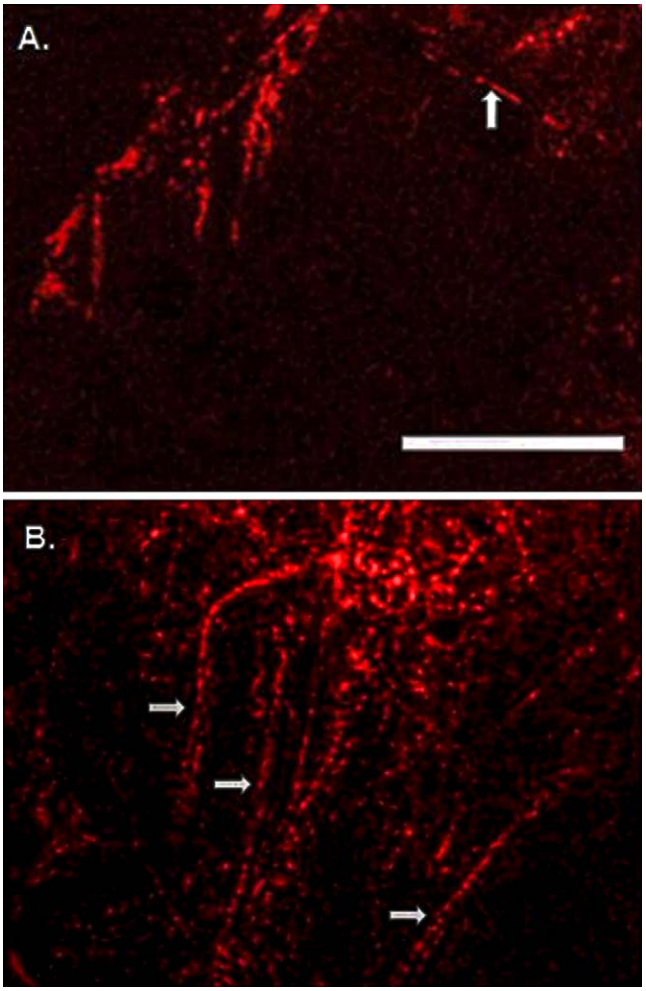

Figure 5. Representative confocal images of porcine conjunctiva/sclera immunostained for the blood vessel-specific antigen CD31, and treated with timolol maleate in the absence (**A**) or presence (**B**) of Y-27632 (1% w/v). *Arrows* indicate blood vessels. *Magnification*: ×10, *scale bar*: 50 µm.

reduction in timolol ocular tissue concentration at 4 hours. A separate cohort of NZW rabbits received treatment with the vasoconstrictor, phenylephrine, prior to subsequent pretreatment with Y-27632 in one eye and treatment with timolol maleate in both eyes at time zero (Fig. 7). Rabbits were next sacrificed at 1 and 4 hours and ocular tissues were collected for drug content. The pharmacokinetic profiles of timolol obtained were similar to those observed in the previous experiment (data not shown). As with the previous experiment, ocular tissue concentrations of timolol of animals pretreated with Y-27632 eyes were divided by the contralateral eye not pretreated with Y-27632 eyes. In the aggregate, there was an approximately 0.12-fold increase in timolol ocular tissue concentration among the three tissues at 1 hour and an approximately 0.06-fold reduction in timolol ocular tissue concentration at 4 hours.

Discussion

ROCK inhibition continues to be an intriguing mechanism for the treatment of elevated IOP associated with POAG.[10–16] Many pharmaceutical companies are presently pursuing active research programs intended to bring a ROCK inhibitor into the marketplace for treatment of POAG.[17] Consequently, the physiological and clinical effects of ROCK inhibitors have been extensively studied. It is postulated that the IOP-lowering effects of ROCK inhibitors is primarily due to enhanced paracellular outflow of aqueous humor through the TM. This is due, in part, to the ability of ROCK inhibitors to relax the cytoskeleton and alter the morphology of the TM at the cellular level and increase the permeability of the inner wall of the Schlemm's canal.[21–23] Further, ROCK inhibitors have been shown to be potent vasodilators, which has made them attractive candidates in the treatment of certain cardiovascular diseases like hypertension and vasospasm.[1–9]

The barriers to intraocular penetration of any administered drug are extensive.[25,26] The cornea itself is exquisitely designed to exclude the penetration of drugs. Furthermore, precorneal barriers to absorption include processes such as tearing and concomitant washout of the drug through the nasolacrimal drainage system. In addition, an extensive conjunctival vasculature can readily absorb administered drugs and carry them away via systemic circulation before intraocular penetration is even achieved. The cellular and physiological consequences of ROCK inhibition on these ocular barriers and

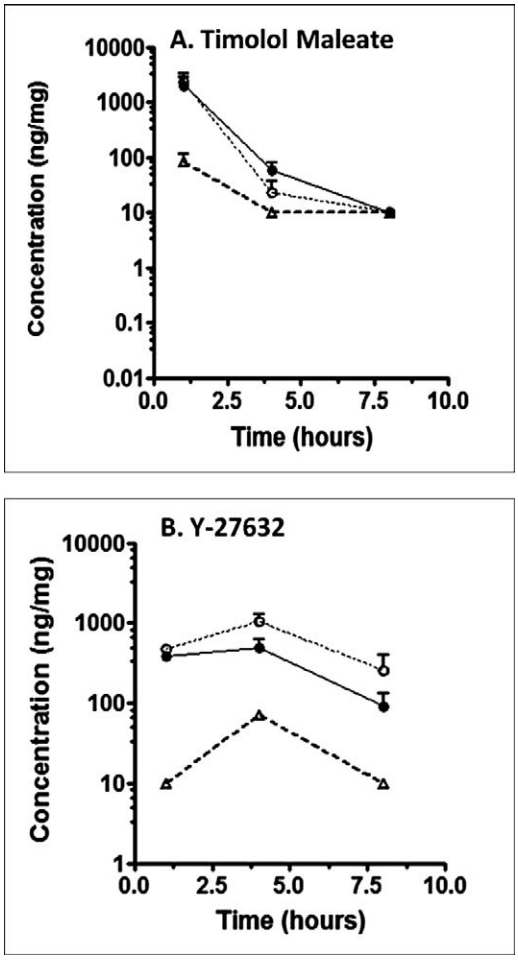

FIGURE 6. Intraocular tissue drug concentrations (ng/mg) of timolol (**A**) and Y-27632 (**B**) after topical administration. Timolol maleate 0.5% w/v eyedrops were administered 10 minutes following pretreatment with Y-27632 1% w/v eyedrops in NZW rabbits. Intraocular tissues evaluated for drug concentrations were iris (*open circle*), aqueous humor (*closed circle*), and lens (*open triangle*). Data are expressed as mean ± standard error of the mean ($n = 4$ eyes at each time-point).

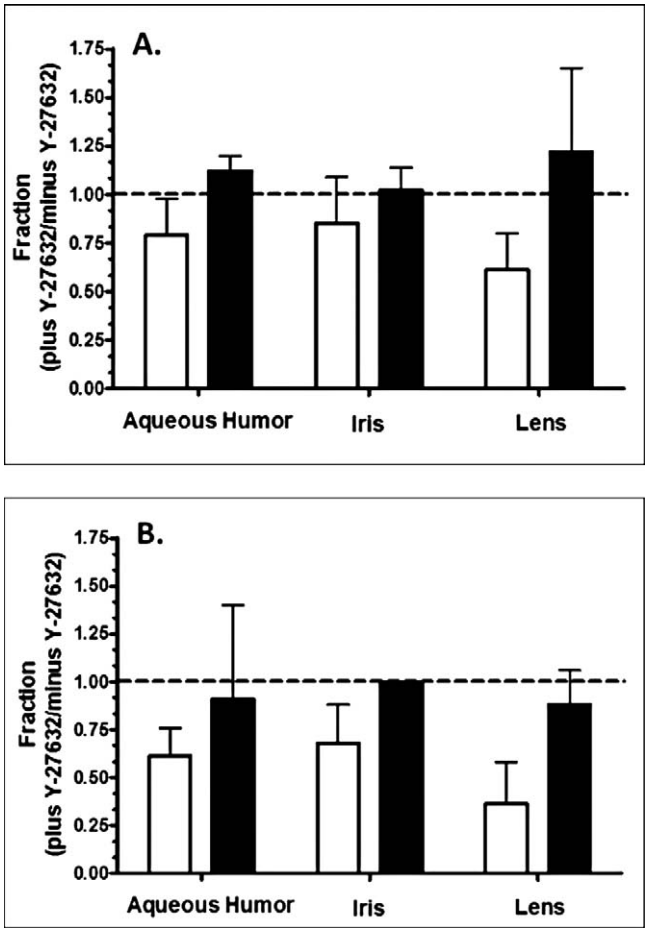

FIGURE 7. Fraction of timolol tissue concentrations found in the intraocular tissues (aqueous humor, iris, lens) of NZW rabbits pretreated with Y-27632 divided by timolol tissue concentrations not pretreated with Y-27632 at 1 hour (**A**) and 4 hours (**B**) (*open bars*). *Closed bars* represent timolol tissue concentrations at 1 hour and 4 hours measured from a separate cohort of rabbits receiving pretreatment with phenylephrine prior to subsequent treatment with Y-27632 and timolol maleate. Data are expressed as mean ± standard error of the mean ($n = 3$–4).

their effect on concomitantly administered ocular hypotensive medications require elucidation.

Initially, the effect that ROCK inhibition might have on the corneal penetration of two clinically marketed ocular hypotensives was assessed in Franz diffusion cells (Fig. 3). It was our initial hypothesis that the physiological action of ROCK inhibition to enlarge the paracellular pathway could lead to increased corneal penetration of concomitantly administered drug. However, it appeared that inclusion of Y-27632 in the donor compartment with either timolol maleate or brinzolamide had very little effect on their eventual penetration across the cornea in the ex vivo diffusion study. In the presence of Y-27632, the overall corneal penetration of timolol maleate decreased within normal variation while the overall corneal penetration of brinzolamide increased within normal variation. Additionally, a similar diffusion cell experiment was conducted with sotalol hydrochloride (Fig. 3). Sotalol is a highly hydrophilic drug which primarily penetrates the cornea via the paracellular pathway, which we initially believed could be loosened sufficiently to affect corneal drug penetration by Y-27632 inhibition. However, the overall corneal penetration of sotalol increased only within normal variation. The lack of a dramatic effect on the corneal penetration of these drugs would not be expected to be due to a short contact time of the ROCK inhibitor with the cornea as would be seen in vivo. Indeed, the design of the Franz cells allows for continuous exposure of the drugs for the entire period of the experiment. A potential explanation for these findings is that ROCK inhibition is sufficient to increase aqueous outflow from the anterior chamber because small changes in the cellular shape of TM cells are adequate to dramatically change fluid flow. However, for drugs, even of a small molecular size, the cellular effects of ROCK inhibition that occur in the anterior chamber on TM cells are not sufficient when applied to corneal epithelial cells to alter morphology and subsequent drug penetration patterns through the paracellular pathway.

An in vivo experiment was conducted to further clarify the effects of ROCK inhibition on the overall ocular barrier to drug absorption. The Franz diffusion cells can be utilized to isolate and examine the effects of ROCK inhibition on the corneal permeability barrier. However, the complete ocular permeability barrier, including cornea, nasolacrimal drainage, and conjunctival circulation, can only be replicated in vivo. NZW rabbits were pretreated in one eye with Y-27632. Afterward,

the animals were treated in both eyes with timolol maleate. This experimental design allowed for the comparison of intraocular tissue concentrations of timolol maleate in pretreated as well as untreated contralateral eyes of the same animals. As noted in Figure 7, reductions in the intraocular tissue concentrations of timolol maleate were observed in those animals pretreated with Y-27632. This reduction in ocular tissue concentration of timolol maleate could be due to some alteration in intraocular clearance or extraocular clearance of the drug. Certainly, the increase in aqueous humor outflow modulated by ROCK inhibition cannot be completely excluded as a significant factor in the rapid clearance of timolol noted in the treated animals. Indeed, future experimentation in our laboratory will seek to ascertain how the intraocular clearance pattern of timolol is affected by ROCK inhibition. However, another extraocular factor could contribute to the reductions in intraocular tissue concentrations of timolol maleate noted in the present experiment. Substantial evidence from the literature supports the ability of the ROCK inhibitors to potently dilate blood vessels including the conjunctival vasculature. Indeed, evidence from experiments conducted in Franz diffusion cells with conjunctiva and sclera tissue herein suggests that Y-27632 has a marked vasodilatory action on conjunctival vasculature (Figs. 4, 5). Such an action in vivo would be expected to dramatically increase blood flow to the extraocular cavity and quickly and efficiently remove concomitantly administered drug like timolol maleate before it can even be absorbed. Previous evidence from the literature has demonstrated that decreasing conjunctival bloodflow pharmacologically with the vasoconstrictor, phenylephrine, could significantly decrease the systemic absorption of timolol.[32,33] Indeed, in a subsequent experiment when a separate cohort of NZW rabbits were pretreated with phenylephrine this proposed increase in timolol clearance due to conjunctival vasculature vasodilation by ROCK inhibition was ostensibly reversed (Fig. 7). This finding highlights the ability of the extensive conjunctival microcirculation to rapidly clear drug from the extraocular cavity which ROCK inhibition augments by promoting vasodilation.

Conclusions

It is expected that ROCK inhibition will have little or no effect on the corneal permeability barrier to ocular hypotensive medications. However, this study presents evidence that the intraocular concentrations of timolol maleate were reduced in the presence of ROCK inhibition. Evidence suggests that this may be primarily due to rapid extraocular clearance from the ocular cavity due to conjunctival blood vessel vasodilation and increased extraocular drug clearance.

Acknowledgments

The authors thank Lori Coward and John Higginbotham for their work in the analysis of ocular drug concentrations.

References

1. Shimokawa H. Rho-kinase as a novel therapeutic target in treatment of cardiovascular diseases. *J Cardiovasc Pharmacol*. 2002;39:319–327.
2. Mohri M, Shimokawa H, Hirakawa Y, Masumoto A, Takeshita A. Rho-kinase inhibition with intracoronary fasudil prevents myocardial ischemia in patients with coronary microvascular spasm. *J Am Coll Cardiol*. 2003;41:15–19.
3. Loirand G, Guerin P, Pacaud P. Rho kinases in cardiovascular physiology and pathophysiology. *Circ Res*. 2006;98:322–324.
4. Liao JK, Seto M, Noma K. Rho kinase (ROCK) inhibitors. *J Cardiovasc Pharmacol*. 2007;50;17–24.
5. Mukai Y, Shimokawa H, Matoba T, et al. Involvement of Rho-kinase in hypertensive vascular disease: a novel therapeutic target in hypertension. *FASEB J*. 2001;15:1062–1064.
6. Fukumoto Y, Matoba T, Ito A, et al. Acute vasodilator effects of a Rho-kinase inhibitor, fasudil, in patients with severe pulmonary hypertension. *Heart*. 2005;91:391–392.
7. Ying H, Biroc S, Li W-W, et al. The Rho kinase inhibitor fasudil inhibits tumor progression in human and rat tumor models. *Mol Cancer Ther*. 2006;5:2158–2164.
8. Somlyo AV, Bradshaw D, Ramos S, Murphy C, Myers CE, Somlyo AP. Rho-kinase inhibitor retards migration and *in vivo* dissemination of human prostate cancer cells. *Biochem Biophys Res Comm*. 2000;269:652–659.
9. Mueller B, Mack H, Teusch N. Rho-kinase, a promising drug target for neurological disorders. *Nat Rev Drug Discov*. 2005; 4:387–398.
10. Sugiyama T, Shibata M, Kajiura S, et al. Effects of fasudil, a rho-associated protein kinase inhibitor, on optic nerve head blood flow in rabbits. *Invest Ophthalmol Vis Sci*. 2011;52:64–69.
11. Rao V, Epstein D. Rho GTPase/Rho kinase inhibition as a novel target for the treatment of glaucoma. *Biodrugs*. 2007;11:167–177.
12. Waki M, Yoshida Y, Oka T, Azuma M. Reduction of intraocular pressure by topical administration of an inhibitor of the Rho-associated protein kinase. *Curr Eye Res*. 2001;22:470–474.
13. Honjo M, Tanihara H, Inatani M, et al. Effects of rho-associated protein kinase inhibitor Y-27632 on intraocular pressure and outflow facility. *Invest Ophthalmol Vis Sci*. 2001;42:137–44.
14. Tokushige H, Inatani M, Nemoto S, et al. Effects of topical administration of Y-39983, a selective rho-associated protein kinase inhibitor, on ocular tissues in rabbits in monkeys. *Invest Ophthalmol Vis Sci*. 2007;48:3216–3222.
15. Williams RD, Novack GD, Van Haarlem T, Kopczynski C. Ocular hypotensive effect of the rho kinase inhibitor AR-12286 in patients with glaucoma and ocular hypertension. *Am J Ophthalmol*. 2011;152:834–841.
16. Honjo M, Tanihara H, Inatani M, et al. Effects of rho-associated protein kinase inhibitor Y-27632 on intraocular pressure and outflow facility. *Invest Ophthalmol Vis Sci*. 2001;42:137–144.
17. Chen J, Runyan S, Robinson M. Novel ocular antihypertensive compounds in clinical trials. *Clin Ophthalmol*. 2011;5:667–677.
18. Lu Z, Overgy DR, Scott PA, Freddo TF, Gong H. The mechanism of increasing outflow facility by rho-kinase inhibition with Y-27632 in bovine eyes. *Exp Eye Res*. 2008; 86:271–281.
19. Rao PV, Deng P-F, Kumar J, Epstein DL. Modulation of aqueous humor outflow facility by the rho kinase-specific inhibitor Y-27632. *Invest Ophthalmol Vis Sci*. 2001;42:1029–1037.
20. Rao PV, Deng P, Maddala R, Epstein D, Shimokawa H. Expression of dominant negative Rho-binding domain of Rho-kinase in organ cultured human eye anterior segments increases aqueous humor outflow. *Mol Vis*. 2005;11:288–297.
21. Hall A. Rho GTPases and actin cytoskeleton. *Science*. 1998; 279:509–514.
22. Chrzanowska-Wodnicka M, Burridge K. Rho-stimulated contractility drives the formation of actin stress fibers and focal adhesions. *J Cell Biol*. 1996;133:1403–1415.
23. Kaibuchi K, Kuroda S, Amano M. Regulation of the cytoskeleton and cell adhesion by the Rho family GTPases in mammalian cells. *Annu Rev Biochem*. 1999;68:459–486.
24. Järvinen K, Järvinen T, Urtti A. Ocular absorption following topical delivery. *Adv Drug Deliv Rev*. 1995;16:3–19.

25. Hornof M, Toropainen E, Urtti A. Cell culture models of the ocular barriers. *Eur J Pharm Bipoharm*. 2005;60:207–225.
26. Urtti L, Salminen L. Minimizing systemic absorption of topically administered ophthalmic drugs. *Surv Ophthalmol*. 1993;37:435–457.
27. Yee S. *In vitro* permeability across caco-2 cells (colonic) can predict *in vivo* (small intestinal) absorption in man-Fact or myth. *Pharm Res*. 1997;14:763–766.
28. Vesna Z, Clark J, Martin R, Vaezy S. Ultrasound-enhanced transcorneal drug delivery. *Cornea*. 2004;23:804–811.
29. Toropainen E, Ranta V-P, Vellonen K-S, et al. Paracellular and passive transcellular permeability in immortalized human corneal epithelial cell culture model. *Eur J Pharm Sci*. 2003; 20:99–106.
30. Madsen KM, Applegate CW, Tisher CC. Phagocytosis of erythrocytes by the proximal tubule of the rat kidney. *Cell Tissue Res*. 1982;226:363–374.
31. Bagi Z, Frangos JA, Yeh JC, White CR, Kaley G, Koller A. PECAM-1 mediates NO-dependent dilation of arterioles to high temporal gradients of shear stress. *Arterioscler Thromb Vasc Biol*. 2005;25:1590–1595.
32. Urtti A, Kyyrönen K. Ophthalmic epinephrine, phenylephrine, and pilocarpine affect the systemic absorption of ocularly applied timolol. *J Ocul Pharmacol*. 1989;5:127–132.
33. Kyyrönen K, Urtti A. Improved ocular: systemic absorption ratio of timolol by viscous vehicle and phenylephrine. *Invest Ophthalmol Vis Sci*. 1990;21:1827–1833.